Pure appl. geophys. 159 (2002) 063–090
0033–4553/02/030063–28 $ 1.50 + 0.20/0

Pure and Applied Geophysics

Post-seismic Effects of an *M* 7.2 Earthquake and Microseismicity in an Abandoned, Flooded, Deep Mine

HIROSHI OGASAWARA,[1] YASUTOSHI KUWABARA,[1] TAKAYUMI MIWA,[1]
KUNIO FUJIMORI,[2] NORIO HIRANO[3] and MAKOTO KOIZUMI[3]

Abstract—An *M* 7.2 earthquake took place 67 km southeast of an abandoned mine containing flooded, vertical ore veins at depth of 1 km. Multidisciplinary monitoring of the unweathered country rock within the mine was carried out for a distance of about one kilometer. The *M* 7.2 earthquake was followed by significant post-seismic changes in strain and tilt of $\sim 10^{-6}$, with a self-potential of ~10 mV, and an increase in the water level in the mine of about 10 cm/day. These phenomena continued for several months before returning to pre-earthquake levels. Coseismic elastic deformations were too small to account for the observed post-seismic changes, and have different senses in strain and tilt from the observed post-seismic changes. The contractions in strain and the changes in the electric self-potential and water-elevation rate strongly suggest an increase in pore pressure. An increase in microseismic activity ($M < 0$) was also observed around the flooded, vertical ore veins about 1–2 km from our multidisciplinary monitoring network, when pore-pressure reached a maximum following the *M* 7.2 earthquake.

Key words: Post-seismic effects, flooded vertical vein, induced seismicity, streaming potential, strain, water table.

1. Introduction

Immediately after the *M* 7.2 1995 Hyogo-ken Nanbu (Kobe) earthquake, Japan, the seismicity rate increased to five or six times the usual level in the Tanba area (the ellipse in Fig. 1) northeast of the aftershock zone (DISASTER PREVENTION RESEARCH INSTITUTE, KYOTO UNIVERSITY, 1995, 1996). Increased seismicity was also observed along the Yamasaki fault (Fig. 1) with a strike conjugate to the Hyogo-ken Nanbu earthquake fault (e.g., NISHIGAMI *et al.*, 1995).

One possible cause of these increased seismicity rates is the static, elastic change in stress associated with dislocation along the source fault of the 1995 Hyogo-ken Nanbu earthquake. Assuming a dislocation along the source fault consistent with

[1] Faculty of Science and Engineering, Ritsumeikan University, 1-1-1 Noji Higashi, Kusatsu, 525-8577, Japan. E-mail: ogasawar@se.ritsumei.ac.jp
[2] Graduate School of Science, Kyoto University, Sakyo-ku, Kyoto, 606-8502, Japan.
[3] Research Center of Earthquake Prediction, Disaster Prevention Research Institute, Kyoto University, Gokasho, Uji, 611-0011, Japan.

geodetic data, HASHIMOTO (1995, 1997) calculated the change in the Coulomb failure function (ΔCFF; e.g., STEIN and LISOWSKI, 1983) for faults that might slip along an E-W compressive stress field in western Japan. He found a coincidence between the relatively high ΔCFF and the epicenter of the largest aftershock. He also found that areas of increased seismicity in the Tanba area and along the Yamasaki fault were located in the higher ΔCFF areas. However the ΔCFF was usually small, at less than 0.06 MPa for most of the Tanba area, and less than 0.02 MPa for the Yamasaki fault. In addition, there are some areas where the sense of the ΔCFF does not coincide with the change in seismicity.

We should consider the effect of a passing surface wave to account for such remote seismicity, because such a wave can produce dynamic strain (e.g., OIKE and MATSUMURA, 1985) as large as several μstrain (a few 0.1 MPa) up to several hundred km from the source of the M $\sim$ 7 event (e.g., GOMBERG and BODIN, 1994).

One of the best-studied examples of such seismicity is the 1992 Landers, California, earthquake (e.g., HILL *et al.*, 1993; ANDERSON *et al.*, 1994). GOMBERG (1996) summarized a number of related studies of this earthquake, and GOMBERG and DAVIS (1996) inferred a trigger threshold dependent on strain rate, based upon responses to seismicity at The Geysers geothermal field in California. The remaining problem was to determine a mechanism to considerably delay seismicity, compared with the very short duration of the dynamic strain. Combining the rate-dependent threshold with the rate- and state-dependent frictional constitutive law (e.g., DIETERICH, 1972, 1978; RUINA, 1983), GOMBERG *et al.* (1997, 1998) successfully explained the delayed seismicity as "clock advance," or hastened seismicity as a nonlinear response to a transient stress perturbation for a hypothetical single block-spring model. Unfortunately, transient effects related to pore fluids were not used in their studies to derive a rate-dependent threshold based upon seismicity at The Geysers. There is certainly a considerable volume of water in The Geysers area (e.g., EBERHART-PHILLIPS and OPPENHEIMER, 1984; STARK and DAVIS, 1996), but these researchers had no *in situ* data for strain or pore pressure at the seismicity sources. In contrast, SLEEP and BLANPIED (1992, 1994) and HILL *et al.* (1993) suggested that the effects of pore fluids can play an important role in inducing seismicity, although there have been few *in situ* data derived from the vicinity of a seismic source area to address this issue.

In this paper we document post-seismic changes in strain, tilt, self-potential and the underground water table that strongly suggest an increase and subsequent decay in pore pressure following the 1995 Kobe earthquake (M = 7.2) at a distance of 67 km (Fig. 1). These factors were monitored using multidisciplinary sensors deployed in unweathered country rock within the Ikuno mine (OGASAWARA *et al.*, 1992; Figs. 1, 2 and 3), an abandoned, flooded rockburst mine. We also evaluate similar post-seismic changes in strain and tilt observed for a 1984 M 5.6 earthquake 30 km from the mine (TABEI, 1987), in an attempt to decipher the causes of post-seismic changes.

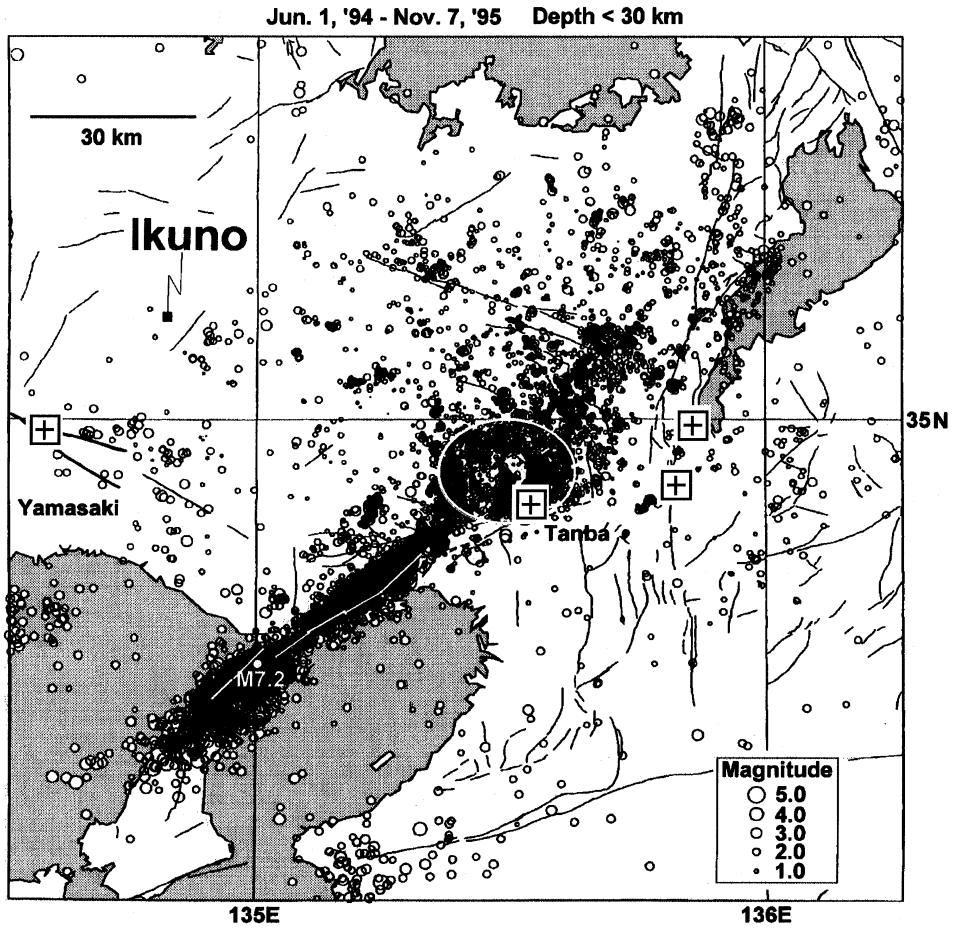

Figure 1

Location of the Ikuno mine (solid square) and the epicenter of the January 17, 1995 Hyogo-ken Nanbu earthquake, Japan (M = 7.2, Japan Meteorlogical Agency; white circle) as well as seismicity ($M > 1$) from June 1994 to November 1995 (DISASTER PREVENTION RESEARCH INSTITUTE, KYOTO UNIVERSITY, 1996). Fault segments (HASHIMOTO *et al.*, 1996) that were activated during the M 7.2 earthquake are shown by white lines. Solid lines show active faults. High seismicity is seen in the Tanba area (indicated by an ellipsoid). Squares with a cross show crustal movement stations where significant change was seen in the secular strain trend. Although no seismicity was detected, several km distant from the Ikuno mine, small and shallow earthquakes ($M < 0$) were observed in the Ikuno mine, as discussed in this paper.

After the abandoned Ikuno mine was mostly flooded, no seismicity was detected nearby the Kyoto University microearthquake observation network, which has a detection threshold of $M > 1$ (Fig. 1). However, microseismicity ($M < 0$) was detected by a small array deployed within the mine (OGASAWARA *et al.*, 1992, 2001; Fig. 4c). The seismicity in the Ikuno mine is shallow (less than a few km deep) and distinct from the surrounding natural seismicity. There have been no mining

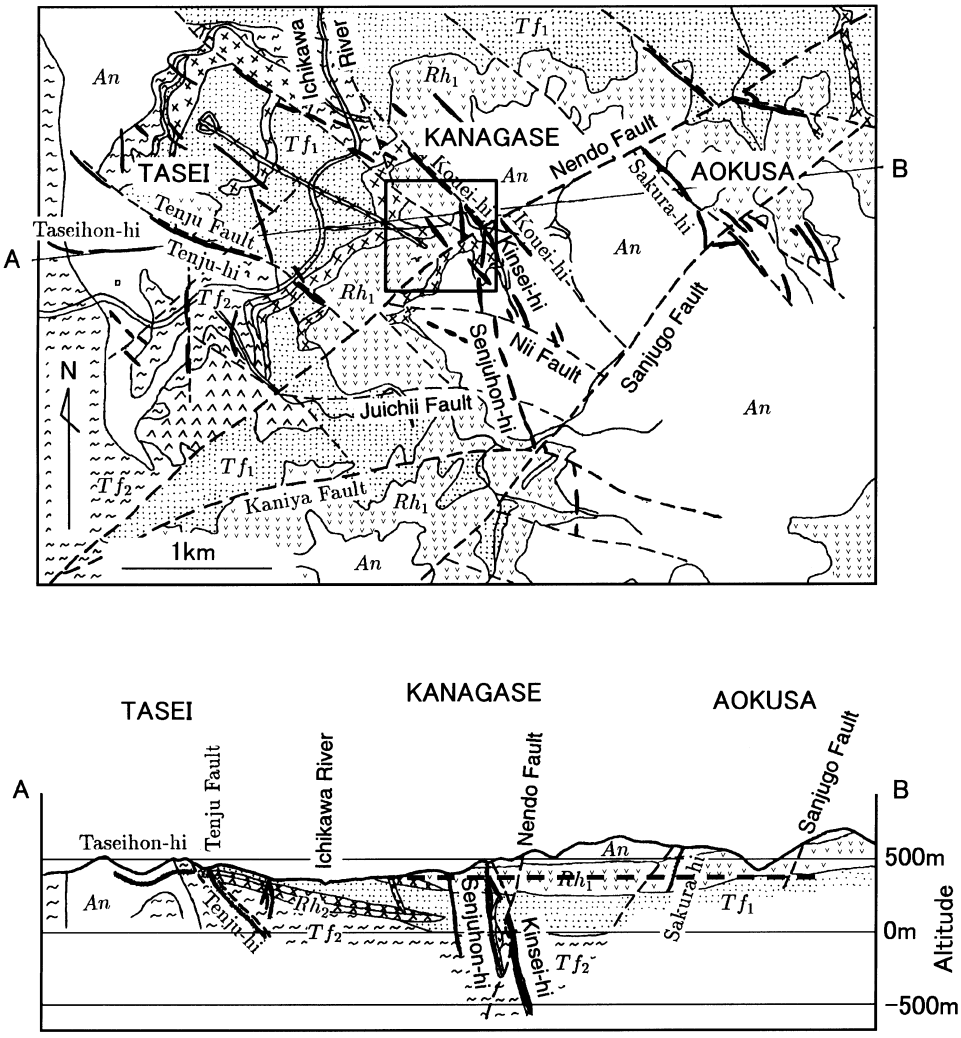

Figure 2

Geology of the Ikuno mine (simplified from the geological map supplied by the Ikuno mine). (Upper) plan view of geology around the Ikuno mine. The Ikuno mine once excavated nearly vertical veins (thick lines) intruded into Tertiary volcanic rocks. The Kanagase area was the most deeply excavated area and experienced rock bursts and water-induced earthquakes. The 750 m × 750 m square in Kanagase is the area where our multidisciplinary observation instruments are installed, as also shown in Figure 3. Dashed lines show geological faults. (Lower) vertical section A-B. A thick, horizontal, dashed line in the lower figure represents the underground level where a geophone array is deployed and a crustal movement monitoring station is located. One of the deepest ore veins was the Kinsei-hi vein where rock bursts occurred. After the Ikuno mine was closed down, the excavated area below the Ichikawa River was flooded, and earthquake swarms were induced in the Kanagase area.

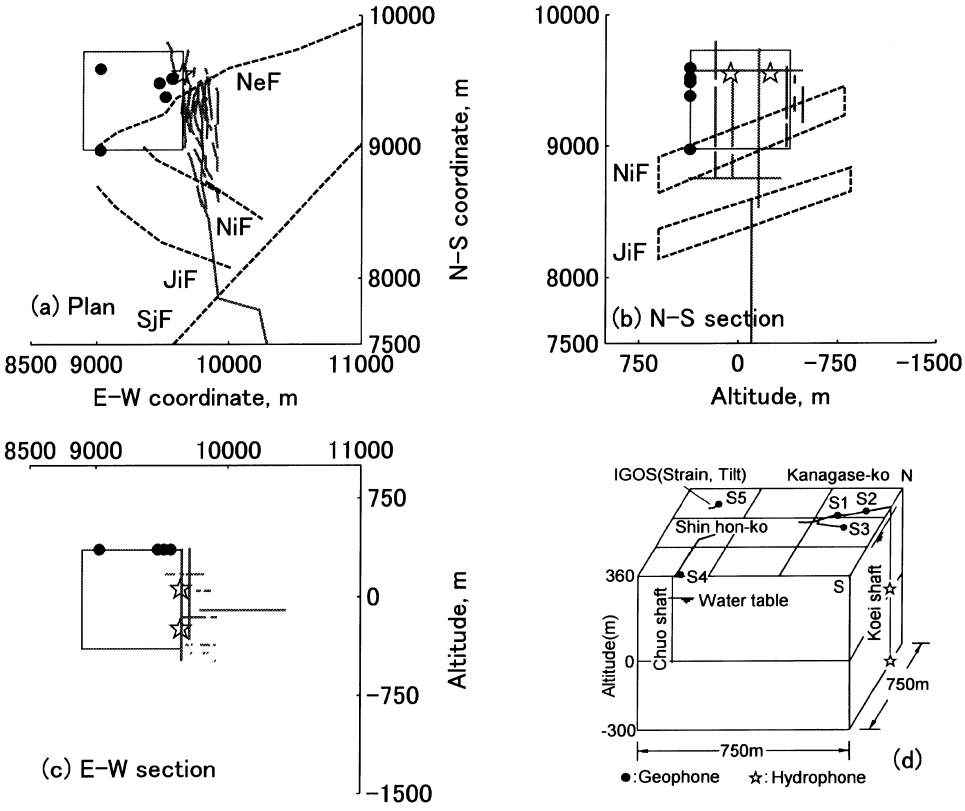

Figure 3

Configuration of the faults, the flooded tunnels at the deep vein, and the monitoring instruments. (a), (b) and (c): Solid and dashed lines are tunnels and faults, respectively. NeF, NiF, JiF and SjF: the Nendo fault, the Nii fault, the Juichii fault and Sanjugo fault, respectively. A square indicates the area where we installed the instruments. Dashed parallelograms in (b) represent fault planes of NiF and JiF projected on the N-S vertical plane. (d): The instrument configuration in the square in (a), (b), (c) and Figure 2 (after OGASAWARA *et al.*, 1992). The table of water flooding the veins was measured at the Koei shaft in the Kanagase area. Significant post-seismic changes were observed using extensometers and tiltmeters at the Ikuno Geophysical Observation Station (IGOS); self-potential was measured by electrodes in the Shinhon-ko (E3-E6) tunnel and in the water table of the Koei shaft.

operations at the Ikuno mine since its closure, and little artificial perturbation that could lead to seismicities. Any seismicity involving the mine is within a few km of our multidisciplinary monitoring network, consequently it is relatively easy to discuss triggers for such seismicity. Seismicities (Fig. 4c) have been associated with a rise of the subterranean water table during heavy rainfall episodes (Fig. 4d; OGASAWARA *et al.*, 2001). However, the Ikuno mine experienced microearthquakes following the Kobe earthquake, even though that time period had the least rainfall of any since we started multidisciplinary monitoring there (Fig. 4e). In this paper we describe the relationship between pore pressure and seismicity at the mine.

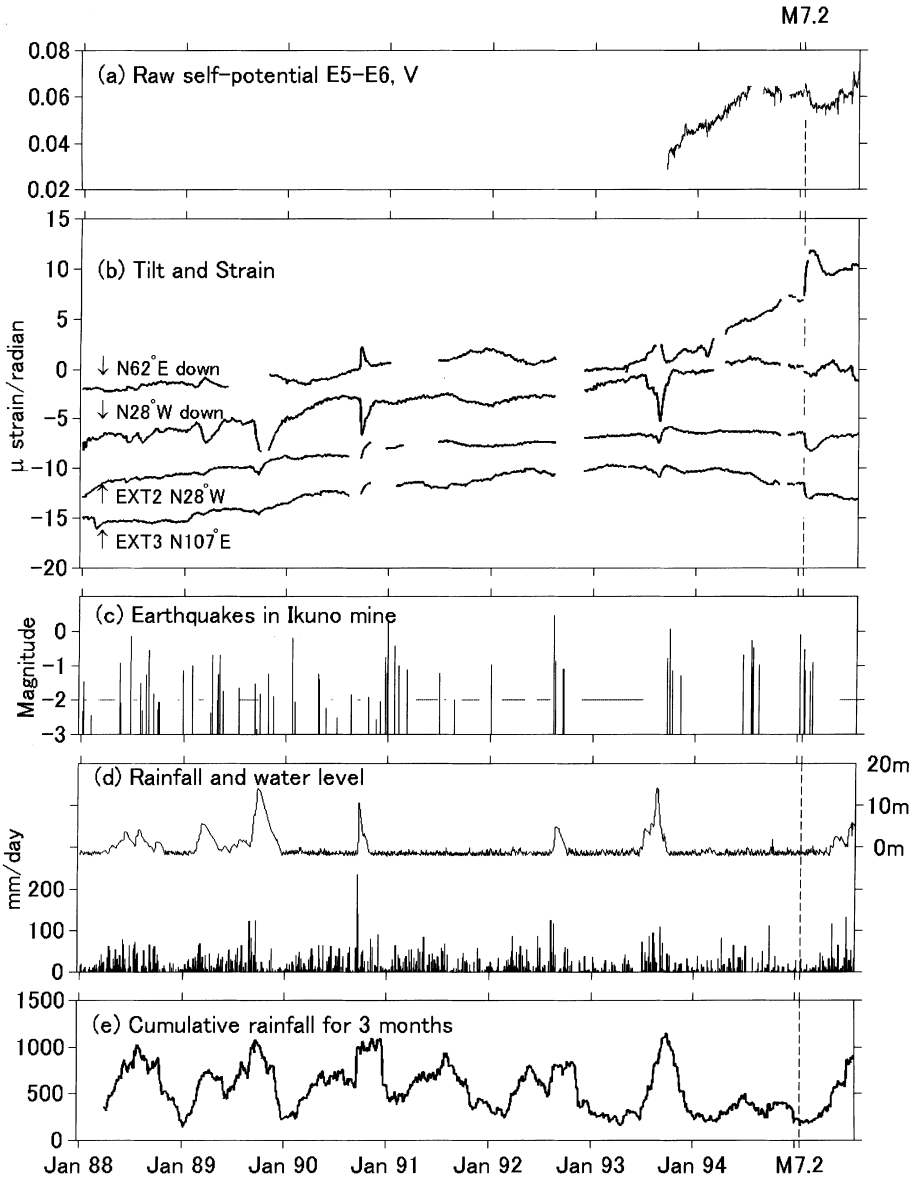

Figure 4

Records of our multidisciplinary observations encompassing an eight-year period. The onset of the *M* 7.2 earthquake is shown by the dashed vertical line. (a): Self-potential of E3-E4. (b): Tilt and strain at IGOS. Arrows indicate direction of downward tilt and extension. (c): Microearthquakes in the Kanagase area. Horizontal lines show time periods without data. (d): Daily rainfall (lower) and water level at the Koei shaft (upper). (e): Cumulative rainfall for the preceding three months.

2. Background

a) The Ikuno Mine and Mine Tremors

The ore veins in the Ikuno mine originated from Tertiary hydrothermal activity. The deepest ore veins are nearly vertical and at a depth of approximately 1 km (Figs. 2 and 3). The mine has a history of induced earthquakes, and the deeply mined, vertical ore veins had rockbursts ($M < 2$) before the mine was closed down in 1973 (TANAKA and NISHIDA, 1971; NISHIDA and TANAKA, 1972). In the late 1970s, the total amount of water flooding the mine reached several tens of millions of tons. The deep veins experienced induced earthquakes ($M < 3$) during this water impoundment (TANAKA and NISHIDA, 1977; TANAKA and OKA, 1979), although seismic activity nearly ceased once the ore veins were mostly flooded. OGASAWARA *et al.* (2001) found that a significant rise of the water table caused by heavy rainfalls activated microseismicity ($M < 0$) around the deepest, flooded, vertical ore veins and around the faults that offset them. They determined that seismicity did not immediately follow the rise in the water table, even though such a rise caused immediate changes in strain and tilt as large as 10^{-6} (Fig. 4b). They concluded that microseismicity does not directly respond elastically to the water load or to the opening of ore veins by the increase in water pressure of about 0.1 MPa. The localized diffusion of the water resulting from the increase in pore pressure may be the cause of the microseismicity.

b) Multidisciplinary Observations at the Ikuno Mine

The monitoring of crustal deformation in the Ikuno mine began in 1943 (SASSA and NISHIMURA, 1951) with horizontal-pendulum tiltmeters placed deep underground. This was followed in 1977 by the installation of extensometers with super Invar pipes, horizontal-pendulum tiltmeters and water-tube tiltmeters at the Ikuno Geophysical Observation Station at an altitude of 360 m (IGOS in Fig. 3d; TABEI *et al.*, 1985). In addition to monitoring crustal deformation, we started multidisciplinary monitoring within the Ikuno mine in 1987 (a thick, dashed, horizontal line in Figure 2 (lower) represents the level of deployment at an altitude of 360 m; OGASAWARA *et al.*, 1992). In order to monitor seismicity, geophones were installed until 1993 on the sidewall at five sites in the tunnels shown in Figure 3d. Hydrophones were temporarily installed in the Koei shaft (Fig. 3d) to check the accuracy of hypocenter locations. As no large station corrections were needed for the geophones and hydrophones, the velocity structure was approximated as homogeneous with $V_p = 4.65$ km/s. The accuracy of hypocenter determination was within several tens of meters until 1993, when a mining museum was constructed underground and we had to suspend seismic monitoring. Beyond 1993, geophone S1 was no longer available and S2 was shifted 200 m to the east, and the accuracy of hypocenter location degraded from several tens of meters to within approximately

one hundred meters. The seismograms were recorded on a PC system with 12-bit, 2-kHz sampling. The detection threshold was $M > -2.5$ before 1993 and $M > -1.5$ after 1993. To monitor self-potential, Pb-$PbCl_2$ electrodes were installed in 1993 in boreholes several tens of cm deep in the footwall of the tunnel, shown as E3–E6 in Figure 3d (OGASAWARA and FUJIMORI, 1995). The Nendo fault (nendo means "clay" in Japanese) is a significant NE-SW-striking, well-fissured fault (Fig. 2) located within several tens of meters of E3 and E5 (compare E3 and E5 with NeF in Fig. 3). The strain, the tilt and the self-potential signals are recorded every five minutes. The level of water in the deep, vertical ore veins at the Koei shaft is measured once a day by an engineer with a tape measure (Fig. 3d). Further details concerning multidisciplinary monitoring and pertaining to the Ikuno mine and the history of induced seismicity are in OGASAWARA *et al.* (2001).

3. The Effects of the M 7.2 Earthquake on the Ikuno Mine

a) M 7.2 Earthquake that Took Place in the Least-rainfall Period

Figure 4e delineates the rainfall pattern over a seven-year period in the Ikuno mine area. It is especially noteworthy that there was little rainfall from the beginning of 1994, and that the M 7.2 event occurred during the lowest period of rainfall. The seismic intensity at the Ikuno mine from the 1995 Hyogo-ken Nanbu earthquake ($M = 7.2$) registered at least 4 on the Japan Meteorological Agency scale (6 or 7 on the modified Mercalli scale).

b) Significant Post-seismic Changes that Cannot be Explained by Coseismic Stress Changes

The strain began immediately after the Hyogo-ken Nanbu earthquake and reached its maximum of about 10^{-6} for every component (Figs. 4b and 5d), which corresponds to an areal contraction of about 2×10^{-6} strain.

►

Figure 5

Significant post-seismic changes for the M 7.2 earthquakes. (a): Electric self-potentials E3-E4 and E5-E6 at Shinhon-ko (Fig. 3d). As unstable drift seen in E5-E6 in January 1995 was removed. E5-E6 with the drift removed and adjusted is shown in (a). (c): Tilt at IGOS. Arrows show directions of downward tilt. (d): Strain at IGOS. Arrows indicate directions of extension. (e): Earthquakes in the Kanagase area. Horizontal line represents a period without data. (f): Rainfall (lower) and the level of water flooding the deep ore veins. Note that microseismic events occurred in the Kanagase area during the period when significant changes were seen in strain and electric self-potential, whereas no significant water table rise or rainfall was seen. We have no available coseismic strain and tilt steps observed for the 1995, because the monitoring system was down for 8 days before the 1995 Hyogo-ken Nanbu earthquake. The strain data after the earthquake are shifted to adjust for this data gap in the layout of this figure.

The GPS network near the Ikuno mine showed no post-seismic displacement larger than 0.5 cm following the Hyogo-ken Nanbu earthquake (GEOGRAPHICAL SURVEY INSTITUTE, JAPAN, 1995). If we divide 0.5 cm by 10^{-6}, the order of the

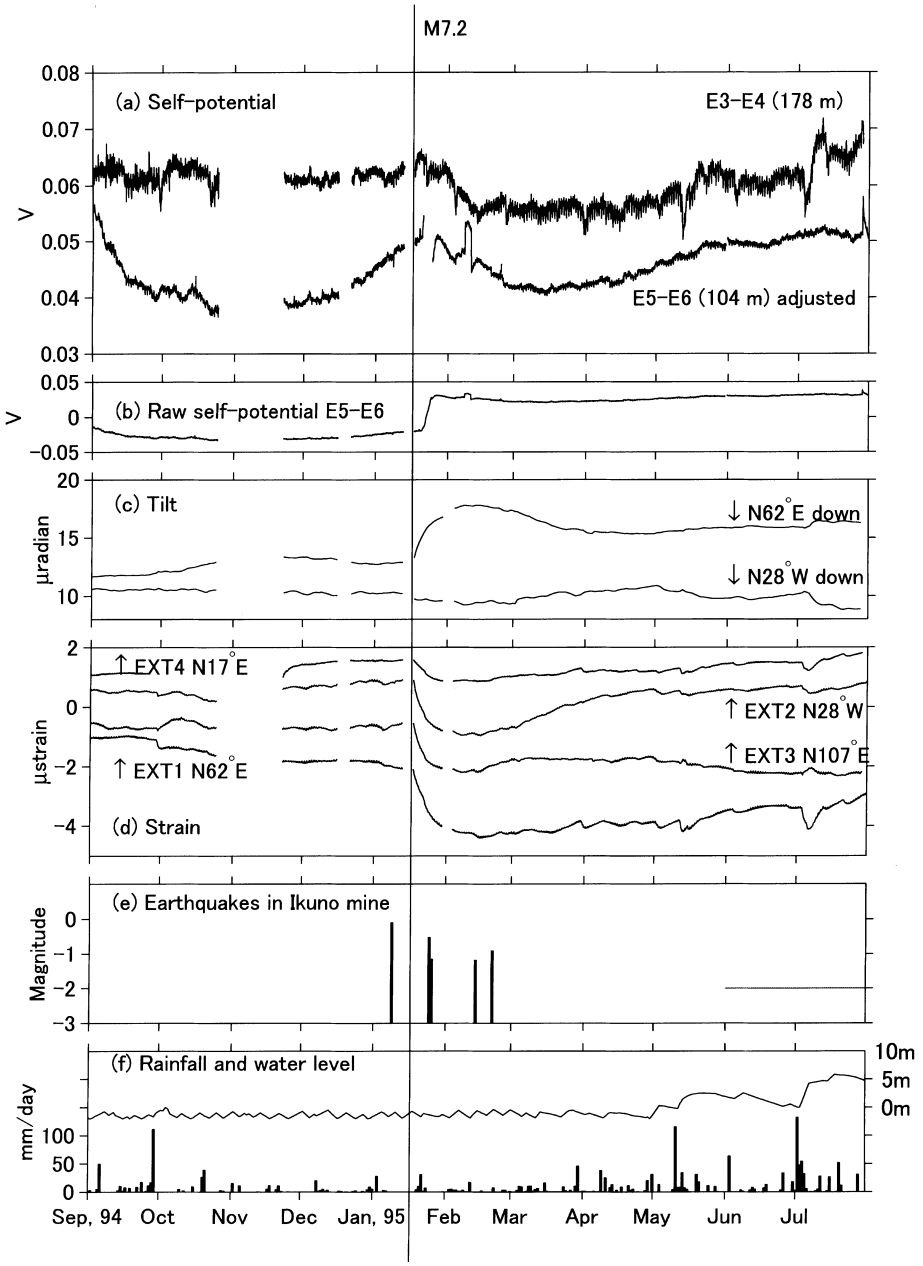

observed strain in the mine, the result is several km, which corresponds to the upper size limit of the area that experienced significant post-seismic deformation. This area is similar to that of the Ikuno mine (Fig. 2), therefore the area which sustained significant post-seismic deformation was confined within the Ikuno mine.

The recording system was not operational for eight days prior to the 1995 Hyogo-ken Nanbu earthquake, therefore we have no available coseismic strain and tilt observations that include this earthquake (Fig. 5). The coseismic strain step can be estimated by computations (e.g., OKADA, 1992) based on the dislocation theory. Assuming fault segments as shown in Figures 1 and 6 (HASHIMOTO *et al.*, 1996), we estimate the coseismic strain and tilt to be as shown in Table 1. The areal strain step at the Ikuno mine from the Hyogo-ken Nanbu earthquake was about 0.3×10^{-6}. The observed post-seismic change in strain corresponds to an areal strain of about 2×10^{-6}, thus the estimated coseismic areal strain step at the Ikuno mine is about one-seventh of the observed value. This value is too small to account for the observed post-seismic change. As shown in Table 1, the characteristics for strain and tilt differ markedly between coseismic and post-seismic changes.

Assuming a reasonable value of the elastic modulus corresponding to the $V_p = 4.65$ km/s used for hypocenter locations (OGASAWARA *et al.*, 2001), the observed post-seismic strain change of about 2×10^{-6} would correspond to a stress

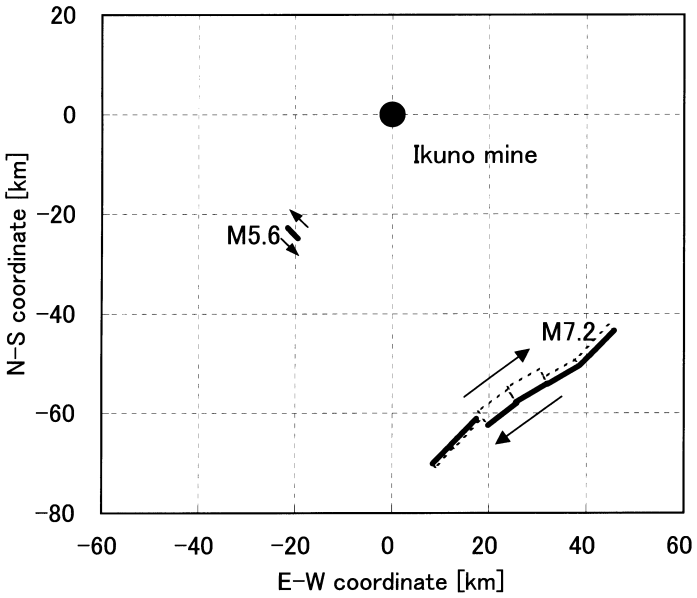

Figure 6
Relationship of the Ikuno mine to two earthquakes (M 5.4 in 1984 and M 7.2 in 1995) that produced significant post-seismic effects at the mine. The M 5.4 event had almost no dip-slip component (after NISHIGAMI and TSUKUDA, 1985), while the M 7.2 event had a significant thrust-slip component as well as a strike-slip component (data after HASHIMOTO *et al.*, 1996).

Table 1

Comparison of coseismic and post-seismic changes in strain (ε) and tilt for M 7.2 and M 5.6 events. Coseismic changes were calculated assuming fault segments shown in Figure 6. Post-seismic changes of M 5.6 are after TABEI *(1987)*

Strain	Coseismic step			Post-seismic change	
	ε_{areal}	ε_{shear}	Comp. axis	ε_{areal}	ε_{shear}
M 5.6 (1984)	-7×10^{-11}	4×10^{-9}	N93°E	-3×10^{-6}	1×10^{-7}
M 7.2 (1995)	-3×10^{-7}	2×10^{-7}	N52°W	-3×10^{-6}	1×10^{-7}

	Tilt	Coseismic step		Post-seismic change	
		Radian	Direction	Radian	Direction
	M 5.6 (1984)	3×10^{-9}	SE-down	2×10^{-6}	SW-down
	M 7.2 (1995)	1×10^{-7}	E-down	6×10^{-6}	SW-down

change of about 0.1 MPa. This is about five times larger than the change in the Coulomb failure function shown on the map published by HASHIMOTO (1995, 1997). In addition, the observed post-seismic contraction suggests an increase in fault strength sufficient to inhibit faulting.

Similar post-seismic strain and tilt changes were observed after an $M = 5.6$ earthquake in 1984 about 30 km to the southwest of the Ikuno mine (TABEI 1987). Figure 7 indicates post-seismic changes in strain versus lapse time (in days) for the main events in 1995 and 1984. Even though the estimated coseismic strain and tilt were quite different between the 1995 and 1984 events (Table 1), the magnitude and duration of the strain changes were surprisingly similar to each other at EXT2 and EXT3. EXT1 and EXT4 were unstable in 1984, which is why we think they were dissimilar. Consequently, the elastic response to the dislocation at the source of the *M* 7.2 and *M* 5.6 events cannot account for the magnitude and the sense of the post-seismic changes in strain or tilt.

c) Self-potential, Indirect Evidence of the Perturbation in the Underground Water System

TABEI (1987) suggested that perturbation of underground water might account for the post-seismic changes in strain and tilt in 1984. However, he had no data available other than strain and tilt values to investigate further.

A clear symptom of perturbation to the underground water system is a post-seismic change in electric self-potential (hereafter SP; KUWABARA *et al.*, 1997a,b). There were gradual changes in SP from September 1993 to June 1994 (Fig. 4a), which we cannot currently explain. However, the post-seismic SP change can be easily distinguished after the onset of the *M* 7.2 event (Fig. 4a).

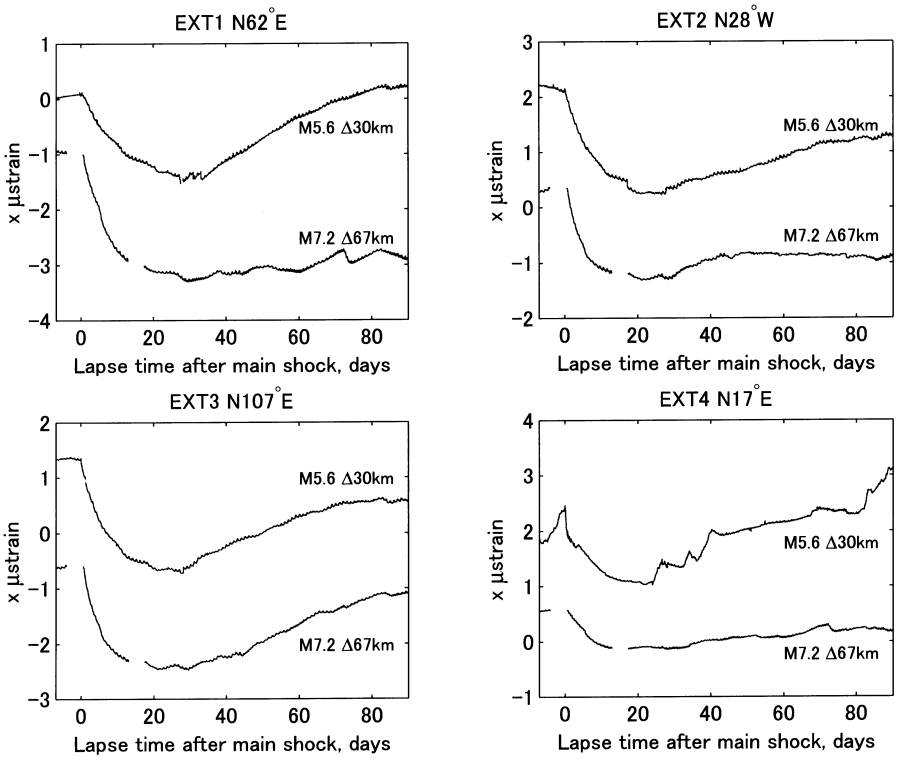

Figure 7
A comparison of post-seismic strain effects for the *M* 5.6 event in 1984 and the *M* 7.2 event in 1995. Strains are plotted versus lapse time after the onset of these events. Note that all are contracted. Regardless of the differences in magnitude and distance from the events, the EXT2 and EXT3 profiles are surprisingly similar to each other. EXT1 and EXT4 are similar, but not so similar as EXT2 and EXT3. We should take them into account that EXT1 and EXT4 were unstable in 1984.

In Figures 5a and 5b the time-axis for post-seismic SP changes is expanded. We had two dipoles, E3-E4 and E5-E6, with the same direction but different spans (Fig. 3d). Since E5-E6 was sometimes unstable (Fig. 5b), we removed the unstable change in E5-E6 in late January 1995 and shifted to the change shown in the lower part of Figure 5a. The differences in high-frequency variation (>10 cycles/day) for E3-E4 and E5-E6 (Fig. 5a) are caused by differences in the span of the dipoles and a remote artificial electric noise source, which suggests that both dipoles detected electric fields well. Independent of differences in the spans of the dipoles, there was a similar magnitude of post-seismic change observed for both dipoles, suggesting that the sources are near E3 and E5. E3 and E5 are installed within 1 m of each other and both are situated within a few tens of meters of the Nendo fault (compare Figs. 3a with 3d). The post-seismic SP change was very slow, compared with the SP changes associated with heavy rainfalls (see May or July, 1995 in Fig. 5 or 7). Rainwater

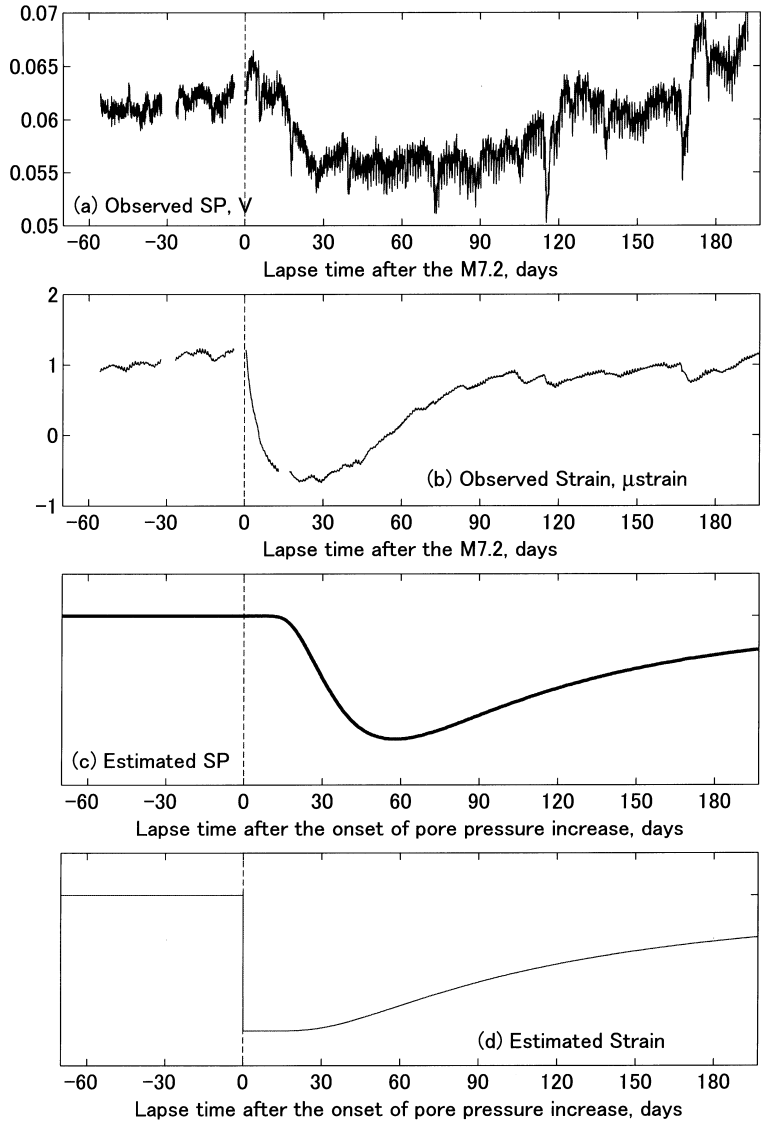

Figure 8

A comparison of post-seismic changes in self-potential and strain. (a and b): Observed SP and strain. (c and d): Theoretically estimated SP and strain, assuming an instantaneous point-source for the pore-pressure increase, a diffusivity, $a = 2 \times 10^{-4}$ m^2/s and a distance, $r = 100$ m. Vertical dotted lines represent the onset of the M 7.2 earthquake and the instantaneous increase in pore pressure. Self-potential and strain are estimated according to Eqs. (1) and (2).Theoretically estimated self-potential (c) and strain (d) explain well the delayed response in self-potential to the onset and instantaneous response of strain to the onset. These also explain well the different recovery processes for self-potential and strain. Therefore, the observed self-potential and strain are strong evidence of a pore-pressure increase, although their variations seem to have different exponential changes with different time constants.

flows rapidly through open fissures near the ground surface, however post-seismic changes are not caused by such rapid water flow.

If we plot SP and strain together (Figs. 8a and b), we see the following characteristics:

(1) The post-seismic change in SP began several days after the M 7.2 earthquake, whereas the strain started immediately after the earthquake. This suggests that the self-potential signal is not caused by a piezo-elastic response to the coseismic stress change of the M 7.2 earthquake. Although the visco-elastic response of a rock mass with some time constant may be able to account for the post-seismic strain and tilt observed immediately after the M 7.2 event, it cannot account for the delay in post-seismic change seen only in the self-potential.

(2) Except for the delay, a change in SP is not the same as a change in strain.

However, these are important evidence that an increase in pore pressure causes both. To demonstrate this, in Figures 8c and d we show self-potential and the strain theoretically obtained by assuming an instantaneous point source for pore-pressure increase, Δp. Since SP is proportional to the gradient of pore-pressure, P (e.g., ISHIDO and MIZUTANI, 1981), for the simplest case, we can assume a point source and SP that can be expressed as:

$$SP \propto \frac{\partial P}{\partial r} = \frac{\partial}{\partial r}\left[\frac{\Delta p}{(4\pi at)^{3/2}}\exp(-r^2/4at)\right] \ , \tag{1}$$

where r is the distance from the source, a the diffusivity and t the lapse time after an instantaneous increase in pore pressure. Associated with Δp, radial stress σ_{rr} is given as:

$$\sigma_{rr} = -\frac{2K_1}{r^3}\left\{\mathrm{erf}\left(\frac{r}{2\sqrt{at}}\right) - \frac{r}{\sqrt{\pi at}}e^{-r^2/4at}\right\} \ , \tag{2}$$

where K_1 is a constant proportional to Δp and the elastic modulus. We find Eq. (2) in textbooks on thermo-elasticity as a response to a point of instantaneous heat (e.g., TAKEUCHI, 1981) and

$$K_1 = (1+\nu)\alpha QG/2\pi(1-\nu) \ , \tag{3}$$

where ν and G are Poisson's ratio and the rigidity, α the thermal expansion coefficient, Q heat instantaneously generated. However, the linearity of the pore-elastic effect is precisely analogous to the theory of linear thermo-elasticity, as RICE and CLEARY (1976) noted. Therefore, Eq. (2) can be used to express temporal change in stress associated with an instantaneous increase in pore pressure at a given point. Figures 8c and 8d show examples of theoretical SP and σ_{rr} that fit better with the observed values (Figs. 8a and 8b), assuming $a = 2 \times 10^{-4}$ m^2/s and $r = 100$ m. We learn from Eqs. (1–2) and Figures 8c and 8d as follows:

– SP is delayed with respect to the onset of pore-pressure increase, whereas strain responds instantaneously to its onset. The distance to the source and diffusivity determine the delay in SP.
– SP starts to recover only after a significant delay, compared to the quick start of recovery of strain. The rate of recovery is determined by the spatial distribution of Δp and diffusivity.

Equations (1) and (2) are Green's functions, thus we can obtain better-fitted profiles by convolving these while considering the space/time variation of Δp. Assuming an instantaneous line or plane source at a distance of $\sim$100 m in a medium with permeability equal to $\sim 10^{-7}$ cm/s and an annual change, KUWABARA (1998) found that the profile which best fits the observed self-potential with a correlation coefficient of 0.88 is shown in Figure 9. Permeability on an order of 10^{-7} cm/s suggests diffusion along the 2nd or 3rd order geological discontinuities' zone (PUSCH, 1995), which is characterized by a fracture zone with a 1–100 m width, 10–1000 m

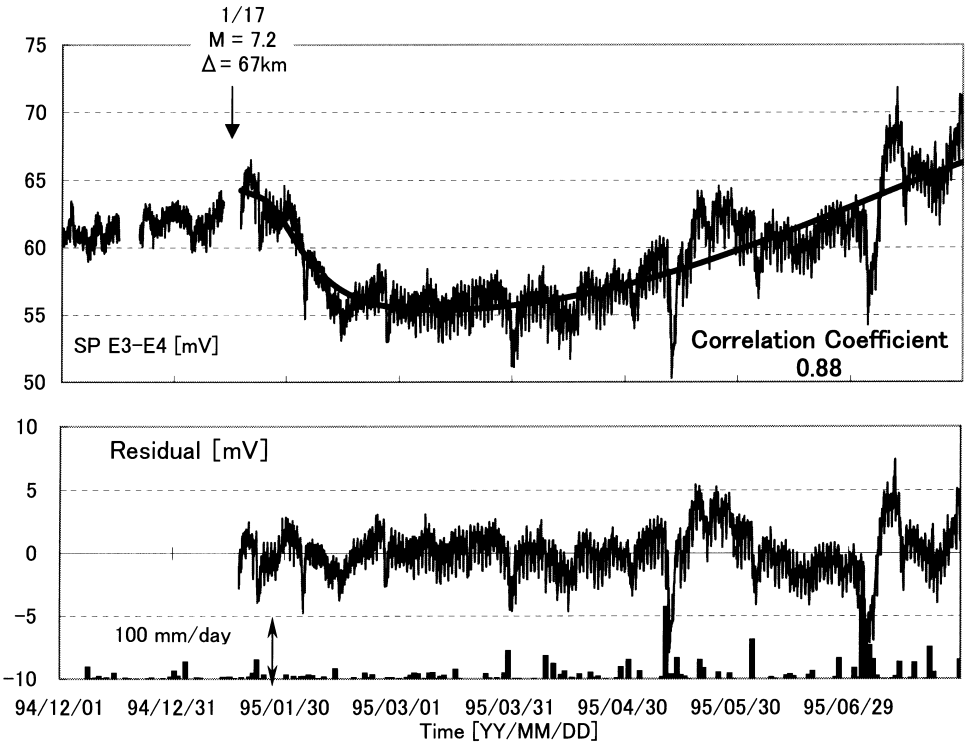

Figure 9
A model to account for the observed post-seismic change in self-potential (after KUWABARA, 1998). (Upper): The observed self-potential and a best-fit model, with a correlation coefficient of 0.88 obtained by assuming a plane source of instantaneous pore-pressure increase and annual change. (Lower): Residuals and rainfall shown by bars.

spacing and 100 m–10 km length. The Nendo faults delineated as thin dashed lines in Figures 3 and 4 are consistent with these ranges. The excavated areas are also candidates, because the 'cut and fill method' was adopted for mining at Ikuno and the underground water diffused through the excavated areas as easily as through the fault zones.

We will not attempt further to find a unique solution to account perfectly for all of the observed strain, tilt and self-potential, because data from only a single station are not enough to fully constrain the solution. However, at least there is a suggestion that Δp did not increase instantaneously, but gradually with time, and reached its maximum in early February. This happened because the observed strain shows a gradual response to the onset (Fig. 8a), regardless of the fact that the theory (Eq. (2), Fig. 8b) predicts an instantaneous strain response to the onset of an instantaneous pore-pressure increase.

d) Direct Evidence: A Significant Change in Water Flooding the Deep Vertical Ore Veins

There is another line of evidence to suggest that the underground water system was perturbed, as reflected in the post-seismic self-potential change. The water level flooding the deep ore veins is usually measured once a day by an engineer at the Koei shaft (Fig. 3d). This water level is controlled by drain pumps so that it does not overflow into the river. Therefore, the water table will rise linearly if no pumps are working, whereas it will drop linearly if either pump is working. As a result, the water table oscillates within a period of several days and a triangular shape with an amplitude of a few m (see the period from November 1994 to March 1995 in Fig. 5f).

It rained briefly before and after the Hyogo-ken Nanbu earthquake on January 17, 1995 (Fig. 4e), and no significant change in the water table at the deep veins was seen as *prima facie* evidence associated with the earthquake (Figs. 4d and 5f); we see only the normal oscillatory changes. However, if we carefully examine the rate of rise for the water table when no pumps were working (the black bars in Fig. 10a; averages are shown by open circles), a jump of about 10–15 cm/day is seen in the elevation rate when the earthquake occurred. We also find a jump in the lowering rate of the water table while the no. 1 or no. 2 pump was working (see gray bars with and without stripes in Fig. 10a, respectively), implying an interesting response. Therefore, in Figure 10b we made plots of a composite water table rate by superimposing the rising/descending rates with respect to those averaged over the period prior to the M 7.2 event. Interestingly, a moving average for seven days (the thick line in Fig. 10b) shows a gradual decrease following the jump, and a gradual recovery from March until heavy rainfall occurred in May. The rate of the water table refers to the flow rate of water that is proportional to the gradient of pore pressure according to Darcy's law, having the same physical response to pressure as the self-potential. As seen in Figure 10b, the composite water table rate (a thick line)

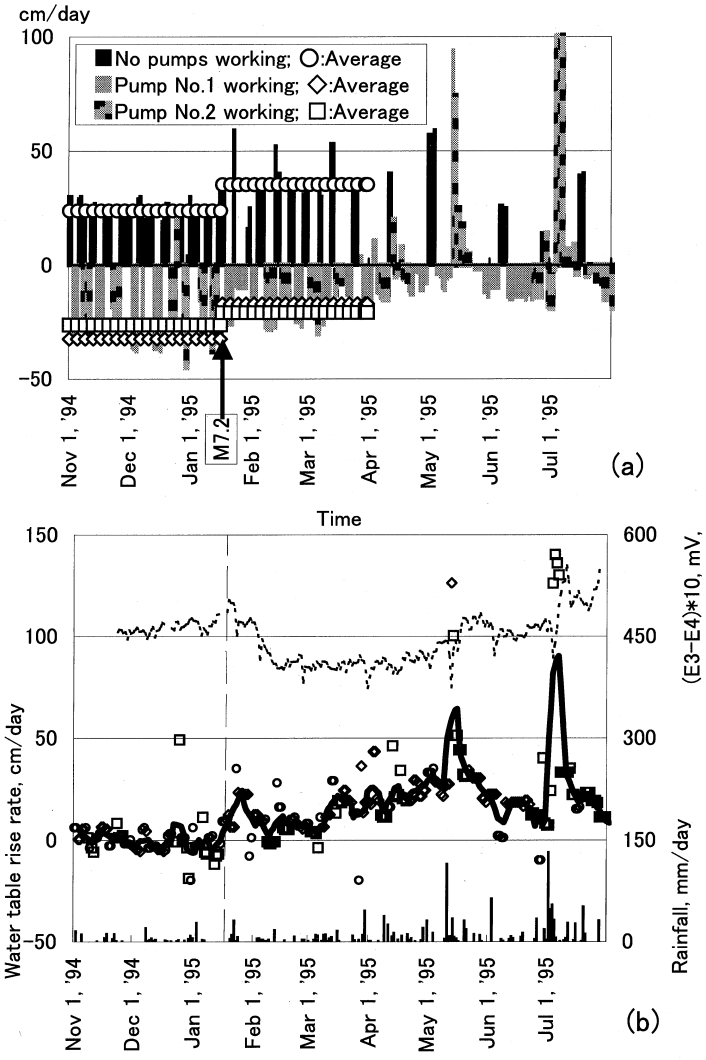

Figure 10

Changes of water level rate flooding the deep ore veins, associated with the *M* 7.2 earthquake. (a): Raw data on water level rate for periods with and without the operation of pumps are shown by bars. Average rates before and after the *M* 7.2 earthquake are represented by circles, diamonds and squares. There are jumps in rate at the onset of the *M* 7.2 event. (b): A composite water level rate. Rates compared to the average for a prior period of the *M* 7.2 are superimposed. A thick line shows the moving average for seven days. Self-potential (dotted line) and rainfall are shown for comparison. The observed self-potential and water level rate are similar from the event's onset to May with abundant rainfall, being consistent with physics that both self-potential and level rate are proportional to the pore-pressure gradient.

looks similar to self-potential (a dashed line), which strongly suggests a close physical relationship between them. Because the water discussed here floods the deep ore veins

in the Ikuno mine, we suggest that pore pressure over the Ikuno mine increased along with the M 7.2 earthquake.

Such minute changes in the water table are seen only during periods with low rainfall. One month before and two months after the M 5.6 event in 1984, it rained considerably more than before and after M 7.2 in 1995. This gives us the rare chance to observe an M 7.2 event during a period of low rainfall, and we were able to distinguish the post-seismic changes independently of any rainfall effect.

e) Earthquake Activity in Ikuno Mine During the Post-M 7.2 Changes

As seen in Figure 5e, there was a swarm of four small earthquakes ($M > -1.5$) following the M 7.2 earthquake. It should be noted that all four small earthquakes occurred in the period of maximum contraction. As discussed in Section 3c, strain directly corresponds to pore pressure, and therefore these fours events occurred in the period with maximum pore pressure and minimum strength.

Figures 11a–11c show the hypocenters of events that occurred before 1993. Diamonds are scaled with lapse times after the onset of heavy rainfalls, and we see that larger diamonds tend to concentrate around deep ore veins (see an area with many deep tunnels in Fig. 11) and around the Nii and Juichii faults that offset the veins (see NiF and JiF in Figs. 11a and b). In Figures 11d–11f the hypocenters of microearthquakes after the M 7.2 event are superimposed as squares. We find that these post-seismic microearthquakes are also located in the area with post-heavy rainfall seismicity. This suggests that these events were also induced by pore-water fluctuation, since it is inferred that post-heavy rainfall seismicity is related to pore-water fluctuation.

However, an event occurred just before the M 7.2 event (Fig. 5e and a triangle in Figs. 11d–11f). In 1994 five events swarmed (Fig. 5e and circles in Figs. 11d–11f) in spite of the relatively low rainfall (Fig. 4e). Certain reasons are needed to explain these earthquakes; otherwise the events following the M 7.2 event appear to be chance phenomena.

Since ten earthquakes occurred during approximately 15 months when there was low rainfall, starting in January 1994, 1.33 ($=2 \times 10/15$) events were expected in a two-month period, with significant post-seismic change. Similarly, by 8.67 events would be expected to occur in the following 13-month period without a post-seismic change. As the observed numbers of events were 4 and 6 for the periods with and without a post-seismic effect, the chi-square is 6.15, which corresponds to a probability of 0.023.

This probability is low but not extraordinarily low. However, here we must consider the coda of the M 7.2 event and the multitude of aftershocks that occurred following it (see Fig. 1). These aftershocks significantly masked small earthquakes in the proximity of the Ikuno mine. In addition, the recording system was frequently interrupted by the dead time for post-trigger processing for every aftershock

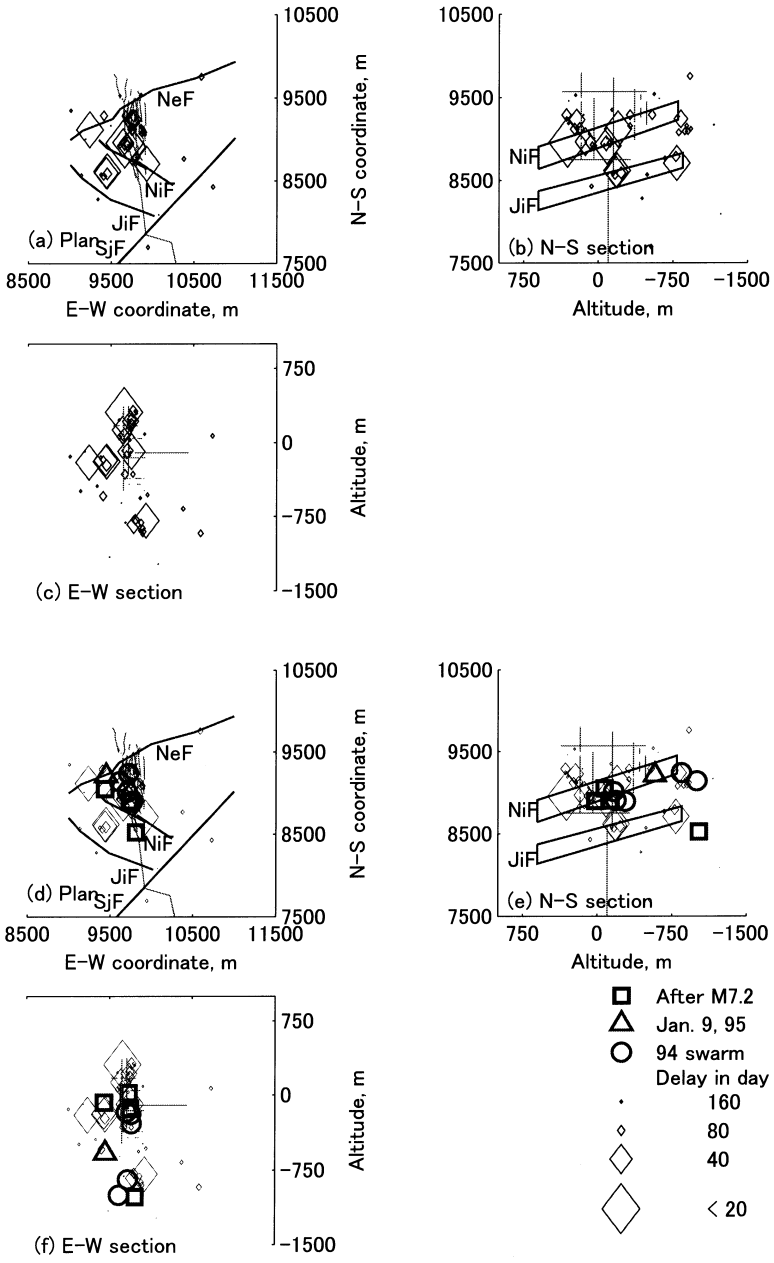

Figure 11

Comparison of hypocenter locations. (a–c): Hypocenters for 56 seismic events before 1993 (after OGASAWARA *et al.*, 2001). Diamonds are scaled with the delay after the onset of heavy rainfall (1988–1992). Thin lines: flooded tunnels in ore veins. Thick lines: faults (NeF, NiF and JiF: Nendo fault, Nii fault and Juichii fault). (d–f): Earthquakes in a low rainfall period in 1994 (circles), an earthquake 8 days before the *M* 7.2 event (a triangle) and the events after the *M* 7.2 event (squares) superimposed on Figures 11(a–c).

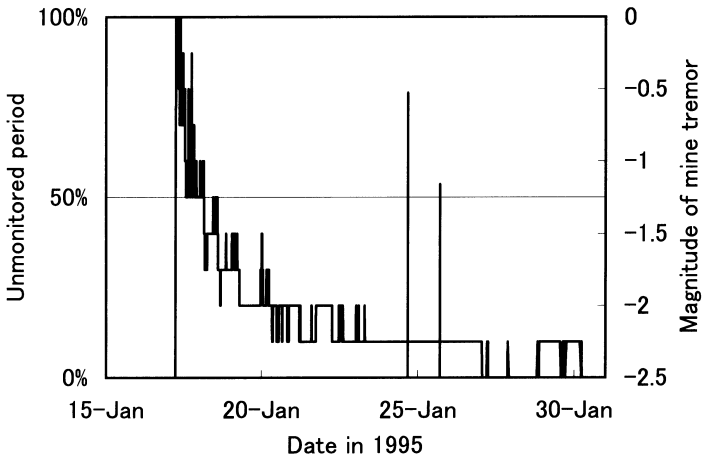

Figure 12
Effect of a coda of *M* 7.2 and frequent aftershocks to microearthquake monitoring in the Ikuno mine. The period when mine events could not be detected is estimated from the relationship between magnitude and the F-P time. The time for post-trigger processing is added to the F-P time to calculate the masked percentage of microearthquake monitoring in the mine. Magnitude data for aftershocks of the *M* 7.2 event (after the Japan Meteorological Agency).

(Fig. 12). There are known instances of microseismicities that immediately followed passage of the seismic wave of large earthquakes (e.g., HILL *et al.*, 1993). Therefore, the possibility exists that more than four seismic events occurred in the vicinity of the Ikuno mine.

The above is only our inference. Accordingly, we will endeauor next to confirm that the two swarms in 1994 and 1995 did not occur by chance. These two swarms took place in 2-month periods, spanning four months. Similar to that noted above, 2.67 events ($=4 \times 10/15$) are expected to occur on average in a 4-month period. However, all ten events swarmed in a 4-month period and no events took place in the other 11-month period. The chi-square for this case is 27.5, which corresponds to a probability of 5×10^{-7}, strongly suggesting that these two swarms did not occur by chance. In addition, the likelihood of 1995 post-seismic seismicity will increase if we can find a good reason to account for the 1994 swarm.

Over an eight-year period we have never had swarms such as those which occurred during the 1994 period of low rainfall. We also find that events in 1994 were located in an area similar to that in which heavy-rainfall seismicity took place. Therefore, we looked for any change that took place only in 1994, and found secular changes that could account for this concurrence of events. There is a clear acceleration to secular change in the S62°W tilt component shown in Figure 4b; it tilted by only a few μradians from 1988 to 1994, and then by several μradians just in 1994. At the same time, as seen in Figure 4b, there was a change in the secular trend in EXT3 with a direction nearly parallel to the E-W tectonic maximum compression;

it expanded from 1988 to 1994 by above five μstrains, whereas it reversed and started contracting by a few μstrain in 1994. Such strain and/or tilt behavior was also observed at other crustal movement stations in the area of Figure 1 (shown as squares with crosses; FURUSAWA, 1995), which depicts seismicity beginning in June 1994 (KATAO and ANDO, 1996). Consequently, we infer that the 1994 swarm at the Ikuno mine was related to a regional change in stress state. Although this is speculative, the swarm may have been caused by the stress change itself or a delayed change in strength associated with a velocity-weakening, as predicted by the rate- and state-dependent friction constitutive law (e.g., DIETERICH, 1972, 1978; RUINA, 1983).

As we could have found an explanation for the 1994 swarm, we speculate that the post-seismic swarm of four earthquakes was related to the *M* 7.2 event or to the significant post-seismic change.

f) Comparison with Post-heavy Rainfall Effects

OGASAWARA *et al.* (2001) noted significant changes in strain, tilt and water table rate following a rise of several m in the water table due to heavy rainfall exceeding several tens of mm/day (Fig. 3). They also documented that the microseismicity in flooded deep ore veins, and on faults that offset the veins, was associated with a significant elevation of underground water. We compare the characteristics of the post-heavy rainfall effect with the post-seismic effect of the *M* 7.2 event, as summarized in Table 2.

The post-*M* 7.2 effects in strain and tilt were similar in magnitude and duration to the post-heavy rainfall effect. However, the direction of the post-*M* 7.2 tilt was nearly orthogonal to the post-heavy rainfall tilt. Contraction with slight shear was observed for the post-*M* 7.2 strain, whereas there was significant shear for the post-heavy rainfall strain. The post-heavy rainfall effects in strain and tilt are well explained by the opening of vertical veins caused by a rise of the water table, but are not necessarily consistent with the faulting mechanisms of microearthquakes induced in the mine. In contrast, the post-*M* 7.2 strain and tilt are well explained by an increase and decay in pore pressure above the mine. Therefore, we infer that the post-*M* 7.2 effect in strain and tilt affected the entire mine, whereas the post-heavy rainfall effect was localized only within deep ore veins.

In contrast, the post-*M* 7.2 microseismicities were seen in a similar location to the post-heavy rainfall microseismicity, namely around the flooded deep veins and the faults that offset the veins.

As discussed above, the post-*M* 7.2 microseismicity was feasibly caused by an increase in pore pressure. However, the post-*M* 7.2 water-table rate was considerably slower than the post-heavy rainfall rate, and in fact was too small to detect during a period of such heavy rainfall. We may speculate on this situation as follows:

Pore-water perturbations that are difficult to sense during heavy rainfall periods can lead to microseismicity in the mine. A significant post-heavy rainfall rise of the

Table 2

Summary of characteristics observed in post-M 7.2 changes and other responses relevant to discussion. O: Similar or comparable, X: different. DWE: dependent upon water elevation

		M 7.2 post-seismic This study	Post-heavy rainfall	
Strain				
	Magnitude	$\sim 2 \times 10^{-6}$	$\sim 1 \times 10^{-6}$; DWE*	O?
	Duration	Several months	Several months; DWE*	O?
	Shear	Little	Significant*	X
Tilt	Magnitude	$\sim 6 \times 10^{-6}$	$<$several $\times 10^{-6}$; DWE*	O?
	Tilt direction	SW-down	SE; Pointing vein*	X
	Duration	Several months	Several months; DWE*	O?
Source of strain and tilt				
		Some broad	Within deep veins	X
Self-potential				
	Magnitude	$\sim$10 mV	Several mV	?
	Duration	Several months	$\lesssim$one month	X
	Delay	Several days	Little	X
Correlation to	strain and tilt	Good but different	N/A	
Correlation to	water table rate	Good and similar	N/A	
Water level				
	Elevation	Less than change by pumping	Several m*	X
	Rate	$\sim$10 cm/day	$\sim$m/day*	X
	Duration	Several months	Depends on pumping*	X
Microseismicity				
	Hypocenters	Near deep veins	Near deep veins*	O
	Active period	A few months after the *M* 7.2 With high pore pressure	A few months after the water table elevation*	O

* after OGASAWARA *et al.* (2001).

water table as large as the post-*M* 7.2 or post-*M* 5.6 increase in pore pressure would act as a trigger to perturb pore water and lead to a decrease in strength, resulting in microseismicity. The post-heavy rainfall perturbation of pore water is localized in deep ore veins, and the perturbation itself is difficult to detect as strain and tilt at IGOS, 1–2 km from the microseismicity hypocenters. However, only significant water table elevation above veins about 1.0 × 1.0-km wide is detectable as associated strain and tilt for heavy rainfall periods.

5. Conclusions

The Hyogo-ken Nanbu earthquake occurred epicentrally 67 km from the Ikuno mine (Fig. 1). The mine had been closed because of rock bursts, and had vertical veins at about 1 km depth flooded after the closure. Significant post-seismic changes

followed the *M* 7.2 earthquake in strain, tilt, self-potential and water table rate in unweathered, subsurface country rock (Figs. 4, 5) despite low rainfall. These changes continued for months before returning to pre-earthquake levels. Both strain and tilt changed in similar ways. The self-potential and the water level rate also changed in similar ways to each other (Fig. 10), although in a different manner from the strain and tilt changes (Fig. 8). Even though these similarities and differences are qualitative, they can be successfully explained by an increase and decay with diffusion of pore pressure, and by physical relationships between strain, self-potential, water-table rate and pore pressure (Fig. 8). In addition, four microearthquakes occurred 1–2 km from our multidisciplinary monitoring network in the mine during a period with maximum pore pressure, which corresponds to minimum strength (Fig. 5).

Post-seismic changes in strain were surprinsingly similar between the *M* 7.2 seismic event in 1995 and the *M* 5.6 event in 1984 (Fig. 7). Nonetheless, the estimated static coseismic strains were quite different and very small for the *M* 5.6 event, compared with the observed post-seismic strain (Table 1). Therefore, we infer that post-seismic change are caused not by static strain change, but probably by dynamic strain from passing seismic waves.

We observed only a small number of microearthquakes in the mine, owing to the triggering threshold of our recording equipment. We lacked continuous seismic records with which we could ascertain if there had been additional small earthquakes in the mine within the coda period of a large event or as aftershocks. We also lacked strong-motion data that would have given us insights of dynamic loading. The parts of the Ikuno mine where we were able to install instruments were very limited because we started our work 15 years after the mine had closed. We hope that these limitations can be addressed in the future. Nonetheless, we must emphasize that we did successfully monitor post-seismic effects during a period of minimal rainfall. Large earthquakes seldom occur, and this was a rare opportunity to study post-seismic effects under these conditions.

The magnitude of the events that occurred in the Ikuno mine was very small. However, they occurred in a limited area during a critical state in a mine that was easy to stimulate seismically. The wider the area over which a critical state prevails, the larger will be the expected magnitude. Although our conclusions are speculative, we still consider that they are applicable to larger natural earthquakes that are shallower than several km. For example, OGASAWARA (2001) carried out an analogous experiment and follow-up numerical analysis to demonstrate that both the power law and exponential decay in seismicity can be explained by transient pore pressure and induced stress. The conditions intrinsic to the Ikuno mine are a large volume of water in a seismogenic zone with open ore veins. Areas with subsurface hydraulic activity contain considerable water and often accompany shallow earthquake swarms. Therefore, we speculate that such areas may be stimulated in a manner similar to the post-*M* 7.2 or post-heavy rainfall effects in the Ikuno mine. A

similar situation prevails where earthquake swarms are associated with upward intrusion of fluid into vertical cracks. For example, earthquake swarms are common off the Izu Peninsula, Japan. These swarms generally accompany significant crustal movement caused by the tensile opening of vertical cracks as wide across as several tens of cms. These cracks are not as narrow as the open veins in the Ikuno mine (e.g., TADA and HASHIMOTO, 1988, 1989; OKADA and YAMAMOTO, 1991). Accordingly we think that multidisciplinary monitoring in mines with flooded, deep veins and induced seismicity is very important to understanding the nature of seismogenic zones under these conditions.

In point of fact, most remote areas (> one fault length) around the M 7.2 event increased in water discharge independent of coseismic static strain (KOIZUMI *et al.,* 1996; Fig. 13), which suggests that pore-pressure increases were common phenomena in many places. However, it is clear that a pore-pressure increase cannot account for the triggered seismicity, if any, in water-poor areas. A number of

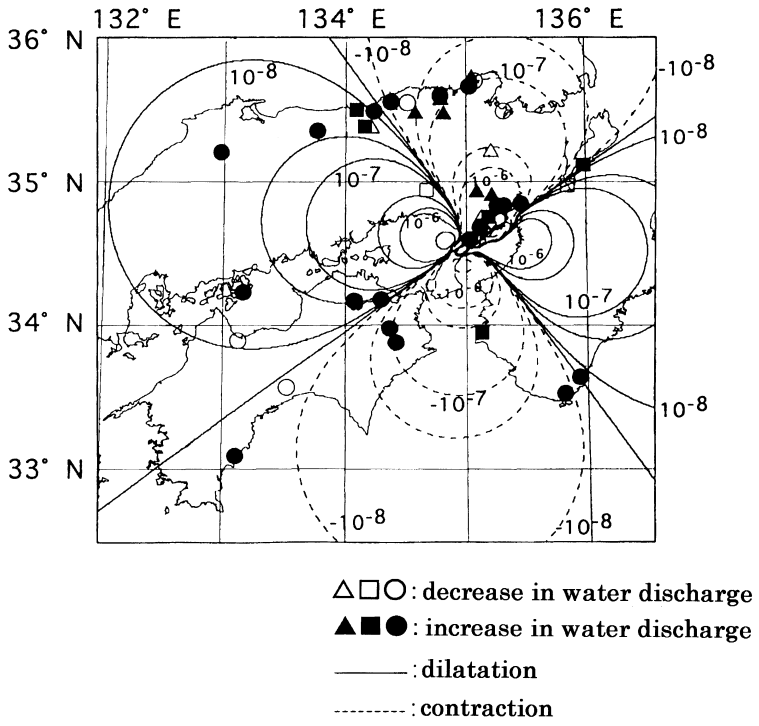

Figure 13
Change in water discharge in hot springs or mineral springs after the 1995 Hyogo-ken Nanbu earthquake (after KOIZUMI *et al.*, 1996). Coseismic volumetric strain change, (thin and thin dashed lines). Solid symbols and open symbols represent increases and decreases in water discharge, respectively. An increase in water discharge was seen at more than 80 percent of the investigated sites, although sites with increased discharge were not necessarily located in the contraction area.

studies have attempted to account for such seismicity under the negligible influence of water (e.g., GOMBERG, 1996; GOMBERG *et al.*, 1998) and some of these studies may possibly apply to same extent in the present case. However, these studies have not considered all possible phenomena, in particular *in situ* data from the immediate vicinity of the hypocentral faults. The typical distance from a surface monitoring station to the hypocenter of a natural earthquake is normally more than 10 km. We think that we will not fully understand the response of the fault to dynamic strain until we have complied *in situ* data from close to the hypocenter of a triggered event. The Research Group for Semi-controlled Earthquake Generation Experiments in South African Gold Mines initiated underground monitoring of normal strain and shear strain several meters from a fault. There is negligible water near this fault, and an event of $M > 2$ is exptected as a result of mining activities (OGASAWARA *et al.*, 2001). Strains reaching 10^{-4} are continuously monitored without clipping, and minute changes are monitored with 24-bit, 25-Hz sampling. This research group expects to obtain interesting *in situ* data, which may allow them to understand not only the response of a fault to dynamic strain, but also the initiation process of an earthquake.

Acknowledgments

We thank Mitsubishi Material Co. Ltd., Silver Ikuno Co. Ltd., and Techno Ohte Co. Ltd. for kindly giving us permission to carry out multidisciplinary observations in the Ikuno mine. We are grateful to Mr. S. Ogata and Mr. H. Matsumoto of Techno ohte Co. Ltd. for kindly supplying us water table data for the Koei shaft and for helping us to conduct our observations. We express our appreciation to Mr. S. Kotani of Mitsubishi Material Co. Ltd. and to colleagues at Kyoto University, who also assisted us to with observations. Comments by Drs. J. Gomberg, I. Beresnev and C. Trifu aided us to greatly improve our manuscript. We thank Prof. M. Yoshida for his help in statistical analysis and Mr. S. Matsuo for his help in preparation of electrodes.

REFERENCES

ANDERSON, J. G., BRUNE, J. N., LOUIE, J. N., ZENG, Y., SAVAGE, M., YU, G., CHEN, Q., and DEPOLO, D. (1994), *Seismicity in the Western Great Basin Apparently Triggered by the Landers, California, Earthquake, 28 June 1992*, Bull. Seismol. Soc. Am. *84*, 863–891.

DIETERICH, J. H. (1972), *Time-dependent Friction in Rocks*, J. Geophys. Res. *77*, 2690–2697.

DIETERICH, J. H. (1978), *Time-dependent Friction and the Mechanics of Stick Slip*, Pure appl. geophys. *116*, 790–806.

DISASTER PREVENTION RESEARCH INSTITUTE, KYOTO UNIVERSITY (1995), *Activation of Seismicity in the Northern Kinki District*, Rep. Coordinating Committee Earthq. Prediction *54*, 517–521 (in Japanese).

DISASTER PREVENTION RESEARCH INSTITUTE, KYOTO UNIVERSITY (1996), *Seismicity Aroung the Rupture Zone of the Hyogoken-Nanbu Earthquake*, Rep. Coordinating Commettee Earthq. Prediction *55* 508–515 (in Japanese).

EBERHART-PHILLIPS, D. and OPPENHEIMER, D. H. (1984), *Induced Seismicity in The Geysers Geothermal Area, California*, J. Geophys. Res. *89*, 1191–1207.

FURUSAWA, T., *The preceding crustal movement*. In The 1995 Hyogoken-Nanbu Earthquake (ed. Research Center for Earthquake Prediction, Disaster Prevention Research Institute, Kyoto University 1995), pp. 22–24 (in Japanese).

GEOGRAPHICAL SURVEY INSTITUTE, JAPAN (1995), *Crustal Movements in the Kinki District*, Rep. Coordinating Committee Earthq. Prediction *54*, 663–521 (in Japanese).

GOMBERG, J. (1996), *Stress/Strain Changes and Triggered Seismicity Following the M_w 7.3 Landers, California, Earthquake*, J. Geophys. Res. *101*, 751–764.

GOMBERG, J. and BODIN, P. (1994), *Triggering of the M_s = 5.4 Little Skull Mountain Nevada, earthquake with Dynamic Strains*, Bull. Seismol. Soc. Amer. *84*, 844–853.

GOMBERG, J. and DAVIS, S. (1996), *Stress/Strain Changes and Triggered Seismicity at The Geysers, California*, J. Geophys. Res. *101*, 733–749.

GOMBERG, J., BLAMPIED, M. L., and BEELER, N. M. (1997), *Transient Triggering of near and Distant Earthquakes*, Bull. Seismol. Soc. Am. *87*, 294–309.

GOMBERG, J., BEELER, N. M., BLANPIED, M. L., and BODIN, P. (1998), *Earthquake Triggering by Transient and Static Deformations*, J. Geophys. Res. *103*, 24,411–24,426.

HASHIMOTO, M. (1995), *Static Stress Changes associated with the Kobe Earthquake: Calculation of Changes in Coulomb Failure Function and Comparison with Seismicity Change*, Zisin *2*(48), 521–530 (in Japanese with English abstract).

HASHIMOTO, M. (1997), *Correction to Static Stress Changes Associated with the Kobe Earthquake: Calculation of Changes in Coulomb Failure Function and Comparison with Seismicity Change*, Zisin *2*(50), 21–27 (in Japanese with English abstract).

HASHIMOTO, M., SAGIYA, H., TSUJI, H., HATANAKA, Y., and TADA, T. (1996), *Co-seismic Displacements of the 1995 Hyogo-ken Nanbu Earthquake*, J. Phys. Earth *44*, 255–279.

HILL, D. P., REASENBERG, P. A., MICHAEL, A., ARABAZ, W. J., BEROZA, G., BRUMBAUGH, D., BRUNE, J. N., CASTRO, R., DAVIS, S., DEPOLO, D., ELLSWORTH, W. L., GOMBERG, J., HARMSEN, S., HOUSE, L., JACKSON, S. M., JOHNSTON, M. J. S., JONES, L., KELLER, R., MALONE, S., MUNGUIA, L., NAVA, S., PECHMANN, J. C., SANFORD, A., SIMPSON, R. W., SMITH, R. B., STARK, M., STICKNEY, M., VIDAL, A., WALTER, S., WONG, V., and ZOLLWEG, J. (1993), *Seismicity Remotely Triggered by the Magnitude 7.3 Landers, California Earthquake*, Science *260*, 1617–1623.

ISHIDO, T. and MIZUTANI, H. (1981), *Experimental and Theoretical Basis of Electrokinetic Phenomena in Rock-water Systems and its Applications to Geophysics*, J. Geophys. Res. *86*, 1763–1775.

KATAO, H. and ANDO, M. (1996), *Seismicity Before and After the Hyogoken-Nanbu Earthquake*, Kagaku *66*, 78–85 (in Japanese).

KOIZUMI, N., KANO, Y., KITAGAWA, Y., SATO, T., TAKAHASHI, M., NISHIMURA, S., and NISHIDAS, R. (1996), *Groundwater Anomalies Associated with the 1995 Hyogo-ken Nanbu Earthquake*, J. Phys. Earth *44*, 373–380.

KUWABARA, Y. (1998), *The postseismic change of the 1995 Hyogo-ken Nanbu Earthquake Detected at old Ikuno Mine (*Δ = 67 km) and its interpretation, Master's Thesis, Faculty of Science and Engineering, Ritsumeikan Univ. (in Japanese).

KUWABARA, Y., OGASAWARA, H., FUJIMORI, K., and KOIZUMI, M. (1997a), *The changes in Electric self-potential before and after 1995 Hyogo-ken Nanbu earthquake*, Abstracts, International Workshop on Seismo-Electromagnetic, March 3, 1997, Chofu, Tokyo, Japan, pp. 133–134.

KUWABARA, Y., OGASAWARA, H., KOYAMA, T., MIWA, T., FUJIMORI, K., and KOIZUMI, N. (1997b), *Changes before and after the Hyogo-ken Nanbu earthquake detected by multidisciplinary observations at Old Ikuno Mine (*Δ = 67 km), 1997 *Proc. Cond. Anomal. Res. Meeting*, 29–36 (in Japanese with English abstract).

NISHIDA, R. and TANAKA, Y. (1972), *Ground Tremors Caused by Rock Bursts in the Ikuno Mine (continued)*, Disast. Prev. Res. Inst., Kyoto Univ. *15-B*, 43–51 (in Japanese with English abstract).

NISHIGAMI, K. and TSUKUDA, T. (1985), *Occurrence Process of the Earthquake – Symposium on the Yamasaki Fault*, The Earth Monthly. *67*, 43–48 (in Japanese).

NISHIGAMI, K., NAKAMURA, M., YABE, M., WATANABE, K., and MATSUMURA, K. (1995), *Change of Seismicity in the Eastern Chugoku Region after the 1995 Hyogoken-Nanbu Earthquake*, Abstract, Seismol. Soc. Jpn. *2*, A50 (in Japanese).

OGASAWARA, H. (2001), *A Simple Analogue Experiment to Account for a Power-law and an Exponential Decay of Earthquake Sequence*, Pure appl. geophys. *159*, 309–343.

OGASAWARA, H. and FUJIMORI, K. (1995), *Observations of Electric Self-potential at a Closed Old mine*, Tech. Note Natl. Res. Inst. Earth Sci. Disast. Prev. *166*, 177–197 (in Japanese with English abstract).

OGASAWARA, H., FUJIMORI, K., KOIZUMI, N., FUJIWARA, S., NAKAO, S., NISHIGAMI, K., TANIGUCHI, K., OTSUKA, S., HIRANO, N., NISHIDA R., and IIO, Y. (1992), *Comprehensive Observation System at Old Ikuno mine for Earthquake Prediction*, Ann. Disast. Prev. Res. Inst., Kyoto Univ. *35B-1*, 389–400 (in Japanese with English abstract).

OGASAWARA, H., FUJIMORI, K., KOIZUMI, N., HIRANO, N., FUJIWARA, S., OTSUKA, S., NAKAO, S., NISHIGAMI, K., TANIGUCHI, K., IIO, Y., NISHIDA, R., OIKE, K., and TANAKA, Y. (2001), *Microseismicity Induced by Heavy rainfall around Flooded Vertical Ore Veins of 1 km deep*, Pure appl. geophys. *159*, 91–109.

OGASAWARA, H., SATO, S., NISHII, S., ISHII, H., IIO, Y., NAKAO, S., ANDO, M., NAGAI, N., OHKURA, T., CICHOWICZ, A., KAWAKATA, H., KUSUNOSE, K., SATOH, T., CHO, A., SUMITOMO, N, and GREEN, R. W. K. (2000), *Semi-controlled Seismogenic Experiment in South African Deep Gold Mines*, Abst. AGU Fall meeting, EOS, 81, No. 48, F1172.

OIKE, K. and MATSUMURA, K. (1985), *Triggers of Earthquake Occurrence*, Chikyu monthly, *7*, 15–19 (in Japanese).

OKADA, Y. (1992), *Internal Deformation due to Shear and Tensile Faults in a Half Space*, Bull. Seismol. Soc. Am. *82*, 1018–1040.

OKADA, Y. and YAMAMOTO, E. (1991), *A Model for the 1989 Seismo-volcanic Activity Off Ito, Central Japan, Derived form Crustal Movement Data*, J. Phys. Earth *39*, 177–195.

RICE, J. R. and CLEARY, M. P. (1976), *Some basic Stress Diffusion Solutions for Fluid Saturated Elastic Porous Media with Compressible Constituents*, Rev. Geophys. Space Phys. *14*, 227–241.

RUINA, A. (1983), *Slip Instability and State Variable Friction Laws*, J. Geophys. Res. *88*, 10359–10370.

PUSCH, R., *Rock Mechanics on a Geological Base* (Elsevier 1995) p. 69.

SETIN, R. S. and LISOWSKI, M. (1983), *The 1987 Homestead Valley earthquake Sequence, California: Control of Aftershocks and Postseismic Deformation*, J. Geophys. Res. *88*, 6477–6490.

SASSA, K. and NISHIMURA, E. (1951), *On Phenomena Forerunning Earthquakes*, Trans. Am. Geophys. Union *32*, 1–6.

SLEEP, N. H. and BLANPIED, M. L. (1992), *Creep, Compaction and the Weak Rheology of Major Faults*, Nature *359*, 687–692.

SLEEP, N. H. and BLANPIED, M. L. (1994), *Ductile Creep and Compaction: A Mechanism for Transiently Increasing Fluid Pressure in Mostly Sealed Fault Zones*, Pure appl. geophys. *143*, 9–40.

STARK, M. A. and DAVIS, S. D. (1996), *Remotely Triggered Microearthquake at The Geysers Geothermal Field, California*, Geophys. Res. Lett. *23*, 945–948.

TABEI, T. (1987), *On the Postseismic Deformation at Ikuno Immediately after the 1984 Yamasaki Earthquake*, J. Phys. Earth *35*, 225–239.

TABEI, T., FUJIMORI, K., and TANAKA, Y. (1985), *Observation of Crustal Movements at Ikuno (1977–1983)*, J. Geod. Soc. Jpn. *31*, 189–201 (in Japanese with English abstract).

TADA, T. and HASHIMOTO, M. (1988), *On the Cause of Abnormal Crustal Deformation in the Northeastern Izu Peninsula (2) – Magma Chamber and Open Crack*, Abst. Seismol. Soc. Jpn. *1*, 139 (in Japanese).

TADA, T. and HASHIMOTO, M. (1989), *On the Cause of Abnormal Crustal Deformation in the Northeastern Izu Peninsula (3) – Open Crack Model and Activity in the Summer of 1988*, Abst. Seismol. Soc. Jpn. *1*, 41 (in Japanese).

TAKEUCHI, Y. (1981), *Analyses of Thermal Stresses*, Nisshin-Shuppan, Tokyo, Japan, pp. 346 (in Japanese).

TANAKA, Y. and NISHIDA, R. (1971), *Ground Tremors Caused by Rock Bursts in the Ikuno Mine*, Bull. Disast. Prev. Res. Inst., Kyoto Univ. *14-A*, 149–164 (in Japanese with English abstract).

TANAKA, Y. and NISHIDA, R. (1977), *Generation mechanism of rock bursts and microearthquakes induced by water-injection into a deep abandoned mine*, In Proc. *5th Jpn. Symp. Rock Mech.*, pp. 91–96 (in Japanese).
TANAKA, Y. and OKA, Y. (1979), *Generation Mechanism of Rock Bursts and Water-induced Earthquakes Under the Tectonic Stress Field*, Rock Mech. Jpn. *3*, 71–73.

(Received March 16, 2000, revised/accepted October 19, 2000)